THE JOURNAL OF PHYSICAL CHEMISTRY Letters

Letter

Cite This: J. Phys. Chem. Lett. 2020, 11, 374−379

pubs.acs.org/JPCL

Observation of 9-Fold Coordinated Amorphous TiO_2 at High Pressure

Yu Shu,[†] Yoshio Kono,*[,‡,⊥] Itaru Ohira,[‡] Quanjun Li,[§] Rostislav Hrubiak,[†] Changyong Park,[†] Curtis Kenney-Benson,[†] Yanbin Wang,[∥] and Guoyin Shen*[,†]

[†]High Pressure Collaborative Access Team, X-ray Science Division, Argonne National Laboratory, Argonne, Illinois 60439, United States

[‡]Geophysical Laboratory, Carnegie Institution of Washington, Argonne, Illinois 60439, United States

[§]State Key Laboratory of Superhard Materials, Jilin University, Changchun 130012, China

[∥]Center for Advanced Radiation Sources, The University of Chicago, Chicago, Illinois 60637, United States

Supporting Information

ABSTRACT: Knowledge of the structure in amorphous dioxides is important in many fields of science and engineering. Here we report new experimental results of high-pressure polyamorphism in amorphous TiO_2 (a-TiO_2). Our data show that the Ti coordination number (CN) increases from 7.2 ± 0.3 at ∼16 GPa to 8.8 ± 0.3 at ∼70 GPa and finally reaches a plateau at 8.9 ± 0.3 at ≲86 GPa. The evolution of the structural changes under pressure is rationalized by the ratio (γ) of the ionic radius of Ti to that of O. It appears that the CN ≈ 9 plateau correlates with the two 9-fold coordinated polymorphs (cotunnite, Fe_2P) with different γ values. This CN−γ relationship is compared with those of a-SiO_2 and a-GeO_2, displaying remarkably consistent behavior between CN and γ. The unified CN−γ relationship may be generally used to predict the compression behavior of amorphous AO_2 compounds under extreme conditions.

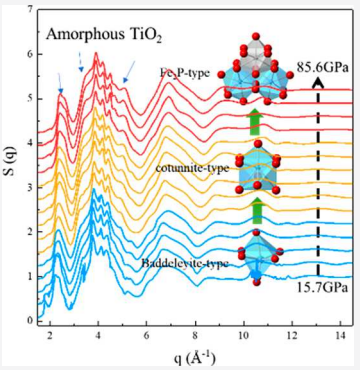

Information about pressure-induced structural changes in amorphous dioxides (a-AO_2) is critical for understanding macroscopic properties (e.g., refractive index, density, elasticity, strength, etc.) under extreme compression. As prototype network-forming glasses, pressure-induced structural changes of amorphous SiO_2 (a-SiO_2) and GeO_2 (a-GeO_2) have been extensively studied.[1−15] At ambient pressure, both a-SiO_2 and a-GeO_2 are characterized by 4-fold coordinated Si and Ge, respectively, forming corner-linked AO_4 tetrahedral networks.[3] Upon compression, the coordination number (CN) of the A cation in a-SiO_2 and a-GeO_2 gradually increases from 4 to 6 at pressures of 18−40 GPa[4−6] and 5−15 GPa,[7−10] respectively. A CN = 6 plateau is reached at ∼40−100 GPa[5] and ∼15−50 GPa[9,11] for a-SiO_2 and a-GeO_2, respectively. Whether additional transformations with CN > 6 can occur under further compression is controversial. X-ray spectroscopy studies show that CNs in a-SiO_2[13] and a-GeO_2[14] remain at ∼6 over wide pressure ranges of 65−120 and 15−100 GPa, respectively. X-ray diffraction (XRD) experiments, however, show continuous and nearly linear increases in CN, with the CNs of a-SiO_2 and a-GeO_2 increasing to ∼7 at 172 GPa[12] and ∼7.4 at 92 GPa,[11] respectively. So far, no CN > 6 plateau has been found in any amorphous dioxides.

TiO_2 is a low-pressure analogue of SiO_2 in studying its high-pressure structural polymorphs.[16] Investigation of amorphous TiO_2 (a-TiO_2) should provide new insight into further CN changes. It is reported that nanograined TiO_2 undergoes pressure-induced amorphization at ∼13−16 GPa,[17,18] with the characteristic structural motifs similar to that of 7-fold coordinated crystalline baddeleyite TiO_2.[17] An *ab initio* simulation study[19] predicts that the CN of Ti in a-TiO_2 gradually increases from 6 to 7 with an increase in pressure up to 55 GPa. Experimentally, however, the pressure corresponding to the change in CN from 6 to 7 is significantly lower[17,18] than those in the simulation.[19] The simulation study also predicts a further change in CN to 8 at 60 GPa, above which CN stays unchanged up to 75 GPa, implying that the next energetically favored structure of a-TiO_2 may have CN = 8.

We compressed TiO_2-B nanoribbons that display amorphization at a pressure range of ∼13.4−16.3 GPa[17] and measured the structure *in situ* using a double-stage large-volume Paris−Edinburgh cell[11] combined with the multiangle energy dispersive X-ray diffraction technique.[20] We found that the CN of Ti of a-TiO_2 continuously increases from 7.2 ± 0.3 at 15.7 GPa to 8.8 ± 0.3 at 70.2 GPa. Over a wide pressure range of 70.2−85.7 GPa, CN remains constant at 8.9 ± 0.3. These results shed new light on pressure-induced polyamorphism in a-AO_2, suggesting that the CN plateau above 6 is 9 for dioxide glasses under extreme compression.

Received: November 15, 2019
Accepted: December 23, 2019
Published: December 23, 2019

DOI: 10.1021/acs.jpclett.9b03378
J. Phys. Chem. Lett. 2020, 11, 374−379

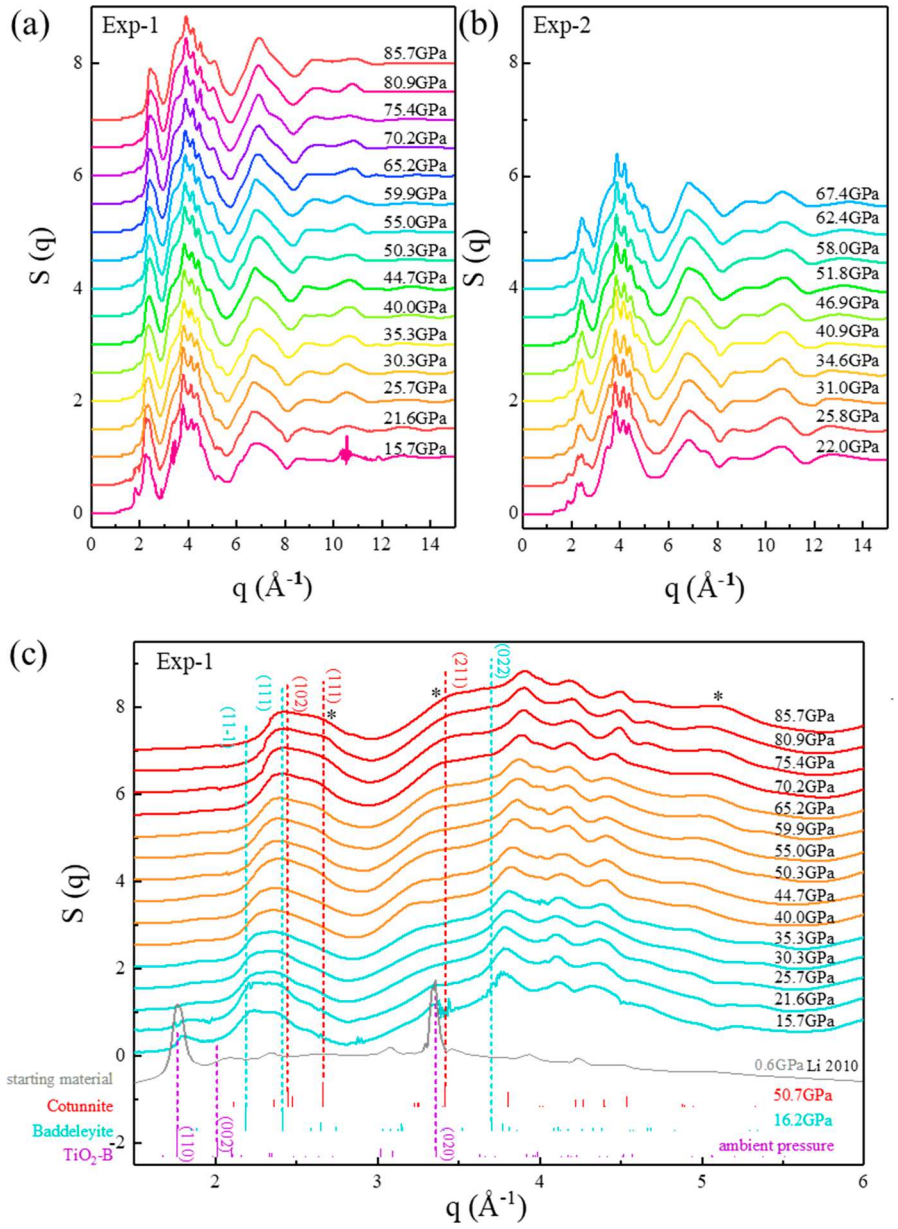

Figure 1. Obtained structure factors $S(q)$ of a-TiO_2 from (a) Exp-1 and (b) Exp-2. (c) $S(q)$ data from Exp-1 (from q = 1.5 to 6 Å^{-1}) are compared with those of the starting material (gray line)[17] and the diffraction peaks of various crystalline polymorphs of TiO_2. Ticks at the bottom indicate peak positions of the crystalline polymorphs: TiO_2-B (purple), baddeleyite (blue), and cotunnite (red). Main peak positions are indicated by long dashed vertical lines. The asterisks indicate the newly formed amorphous peaks under high pressure.

Structure factors, $S(q)$, of a-TiO_2 were determined at pressures of ≤85.7 GPa (Exp-1) and ≤67.4 GPa (Exp-2) in two experimental runs (panels a and b, respectively, of Figure 1). Over the entire pressure ranges, $S(q)$ exhibits five peaks centered around 2.4, 4, 7, 8.5, and 11 Å^{-1}. All of these peak positions are close to the $S(q)$ peaks from a simulation study at ambient pressure,[21] except a small one located around 8.5 Å^{-1}. Three weak nanocrystalline peaks are superimposed on the second amorphous peak at ∼4 Å^{-1}, which persists over the entire pressure range. These peaks correspond to the (023), (−222), and (313) planes of the TiO_2-B phase.[17] As shown in the Supporting Information, the presence of these remaining crystalline peaks does not significantly affect the structural analysis of the a-TiO_2 sample.

At 15.7 GPa, two characteristic peaks near 1.8 and 3.35 Å^{-1}, corresponding to the (110) and (020) planes of the TiO_2-B structure, respectively, were visible (Figure 1c). With an increase in pressure, these two peaks completely disappeared above 30.3 GPa, which is consistent with the result reported previously.[17] The first amorphous peak displays a broad top from ∼2.2 to 2.4 Å^{-1} at 15.7 GPa. This q range corresponds to the interplane distances of (11−1) ($q \approx 2.19$ Å^{-1}) and (111) ($q \approx 2.42$ Å^{-1}) of baddeleyite TiO_2 at 16.2 GPa.[22] With an increase in pressure, the shape of the first peak gradually changed to be asymmetrical. Above 50.3 GPa, a new shoulder appeared at the high q side (∼2.65 Å^{-1}) with its intensity increasing as pressure was further increased. Eventually, above 70.2 GPa, the fist peak developed a new broad top from ∼2.4 to 2.65 Å^{-1} corresponding to the (102) ($q \approx 2.45$ Å^{-1}) and (111) ($q \approx 2.66$ Å^{-1}) planes of the 9-fold coordinated cotunnite TiO_2 at 50.7 GPa.[22] Meanwhile, above 40.0 GPa, two peaks emerged at ∼3.25 and ∼4.95 Å^{-1} with their

DOI: 10.1021/acs.jpclett.9b03378
J. Phys. Chem. Lett. 2020, 11, 374−379

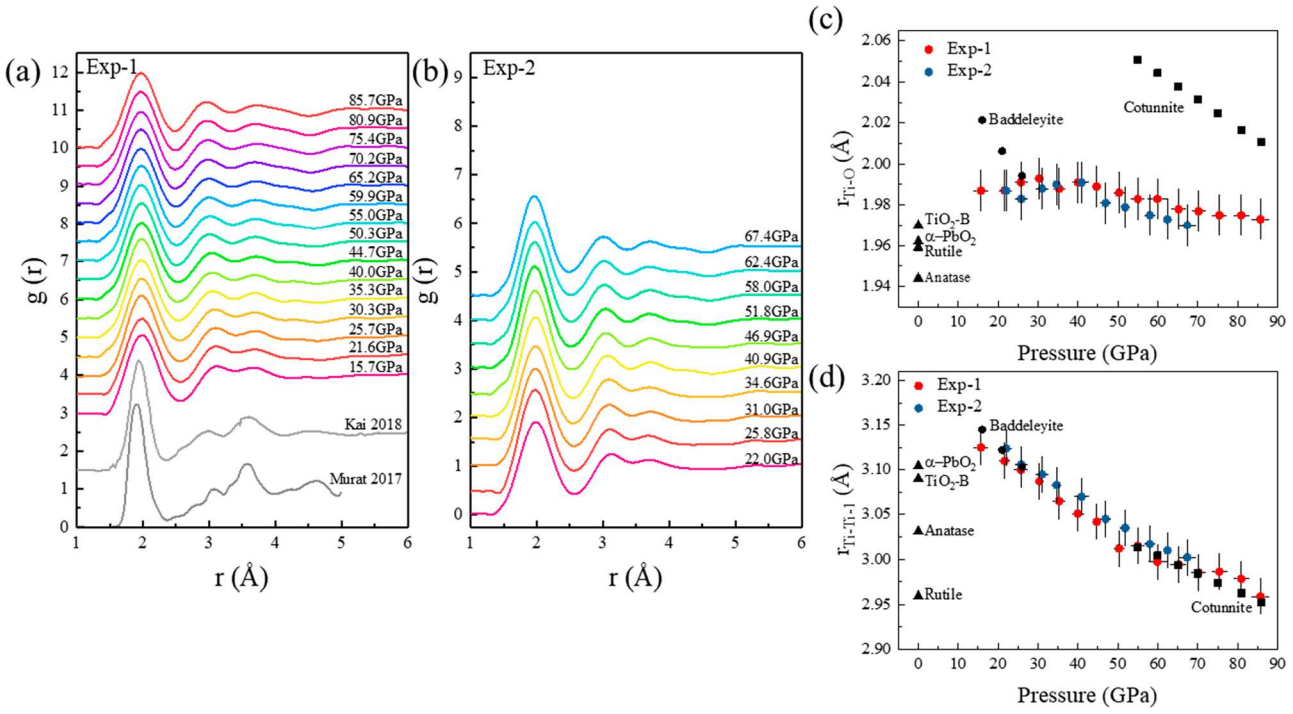

Figure 2. (a) Pair distribution functions $g(r)$ from Exp-1 (colored lines) together with that from simulation at ambient pressure (gray line).[19,21] (b) $g(r)$ from Exp-2. (c and d) Colored circles are r_{Ti-O} and $r_{Ti-Ti-1}$ obtained from the first and second peak positions of $g(r)$, respectively. Black symbols are the calculated average r_{Ti-O} and $r_{Ti-Ti-1}$ of TiO_2 crystalline polymorphs.[22]

positions shifting to high q as the pressure was increased to 70.2 GPa. These changes in $S(q)$ indicate a gradual structural change from 15.7 to 70.2 GPa. At higher pressures from 70.2 to 85.7 GPa, no clear changes in $S(q)$ were observed (Figure 1(c)).

Pair distribution functions, $g(r)$, were derived for a-TiO_2 as shown in Figure 2. The first three $g(r)$ peaks near 1.99, 3.1, and 3.7 Å are assigned to represent Ti−O (r_{Ti-O}), Ti−Ti−1 ($r_{Ti-Ti-1}$), and Ti−Ti−2 ($r_{Ti-Ti-2}$) distances, respectively. The O−O distance (r_{O-O}) expected to be centered roughly around 2.4 Å[19] is barely recognizable. This may be due to (1) the relative weak scattering power of oxygen and (2) the r_{O-O} peak, which decreases rapidly with an increase in pressure, overlapping with the intense r_{Ti-O} peak.[19] All peaks in the obtained $g(r)$ are broader than those from simulations,[19,21] partly because the Lorch modification function was applied in our Fourier transformation process. $r_{Ti-Ti-1}$ and $r_{Ti-Ti-2}$ are attributed to the distances of two Ti atoms with edge-sharing (or face-sharing) and corner-sharing polytopes, respectively.[21] The intensity ratios of the Ti−Ti-1 versus Ti−Ti-2 peaks are reversed when compared to the ambient-pressure simulation $g(r)$ (Figure 2a,b). This suggests that the fractions of edge-sharing and face-sharing interpolytope connections in compressed a-TiO_2 are higher than the 6-fold-coordinated a-TiO_2 at ambient pressure.

Major factors affecting the A−O distance in a-AO_2 under high pressure include compression and local structural changes. Compression tends to decrease the A−O distance, while structural changes, often involving an increase in CN, tend to increase the A−O distance with an increase in pressure. In the latter case, the increased distance is commonly expressed as the increased (apparent) ionic radius for the A cation.[23] Figure 2c shows clearly that the r_{Ti-O} values of a-TiO_2 above 10 GPa are greater than the average ambient-pressure Ti−O distances in 6-fold crystalline structures (TiO_2-B, rutile, α-PbO_2, and anatase),[22] suggesting that the CN of Ti is likely higher than 6. Figure 2c also shows that r_{Ti-O} is more or less constant at ∼1.99 Å between 15.7 and 40.0 GPa, suggesting that the competing effects of compression and structural change nearly cancel each other. Because the effect of compression on Ti−O distance is generally a gradual and smooth process,[17] the CN in a-TiO_2 likely increases gradually with an increase in pressure from 15.7 to 40 GPa. Above 40 GPa, r_{Ti-O} becomes negatively dependent on pressure, from 1.99 Å at 40.0 GPa to 1.97 Å at 85.7 GPa, with a slope much smaller than those of crystalline TiO_2 phases (Figure 2c). The decrease in r_{Ti-O} with pressure suggests that the effect of compression becomes greater than that of the CN change between 40 and 85.7 GPa.

Figure 2d shows that $r_{Ti-Ti-1}$ in a-TiO_2 decreases almost linearly with an increase in pressure. Interestingly, the compression behavior of $r_{Ti-Ti-1}$ in a-TiO_2 is similar to the average edge-sharing Ti−Ti distance of baddeleyite TiO_2 and the average face-sharing Ti−Ti distance of cotunnite TiO_2. Because $r_{Ti-Ti-1}$ represents how closely each TiO_x polyhedron is connected to its neighbors, the compression behavior of $r_{Ti-Ti-1}$ in a-TiO_2 suggests that the interpolyhedron connection in a-TiO_2 may be close to those in the 7- and 9-fold coordinated crystalline structures.

We determined the CN of Ti in a-TiO_2 by fitting the first peak of $g(r)$ with the pair function method[24] (more details in the Supporting Information). The CN was determined to be 7.2 ± 0.3 at 15.7 GPa, and then it quickly increased to 8.4 ± 0.3 at 40.0 GPa (Figure 3a). Upon further compression, the CN increased to 8.8 ± 0.3 at 70.2 GPa and then remained constant around 8.8−8.9 up to the highest pressure of 85.7 GPa. With all of the results from the $S(q)$, $g(r)$, atomic distances, and CNs (Figures 1−3), structural evolution of a-

DOI: 10.1021/acs.jpclett.9b03378
J. Phys. Chem. Lett. 2020, 11, 374−379

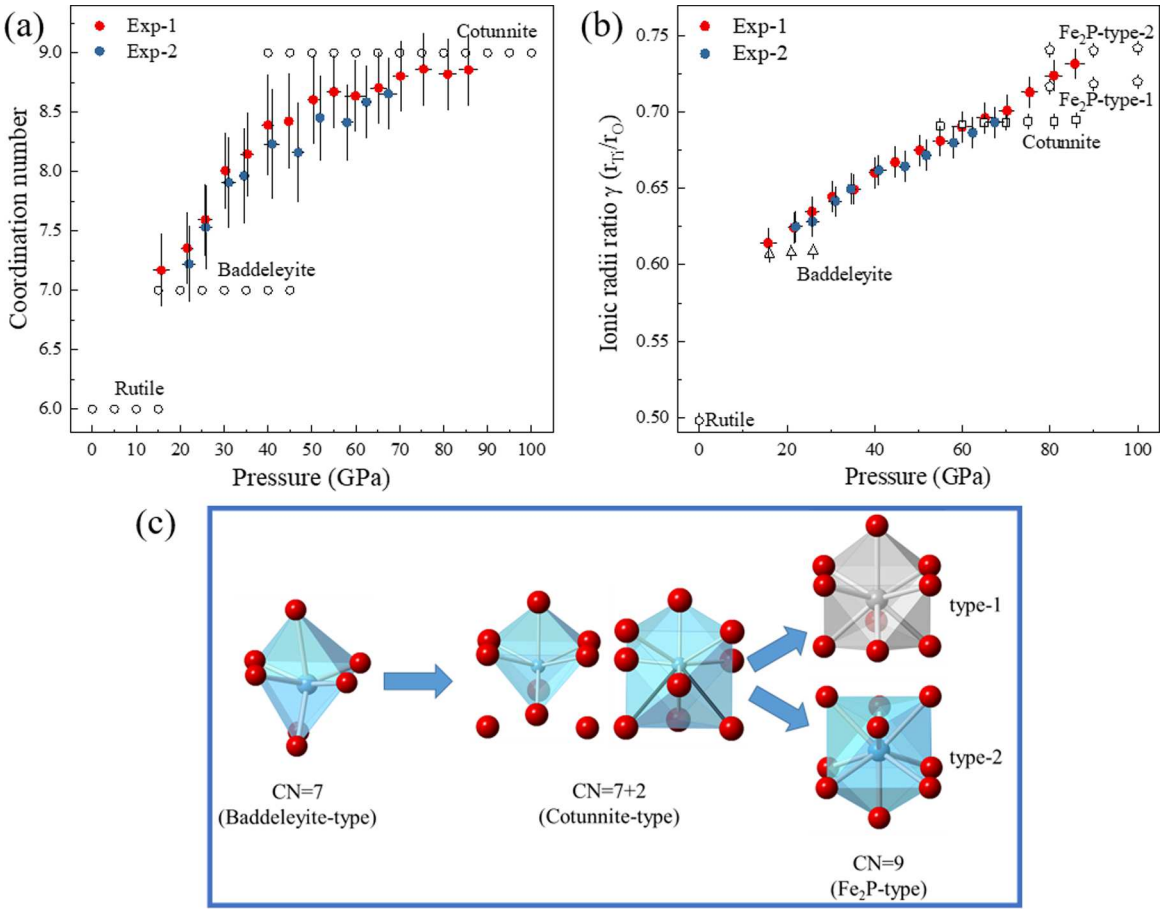

Figure 3. (a) Coordination number (CN) of Ti in a-TiO_2 as a function of pressure. Numerical values of the CN are summarized in the table in the Supporting Information. (b) Ionic radius ratio ($\gamma = r_{Ti}/r_O$) as a function of pressure. Here, a-TiO_2 data (filled circles) are compared with those of TiO_2 crystalline polymorphs (empty black symbols). (c) Schematics showing geometric features of different coordination motifs in crystalline TiO_2. Red and blue spheres represent oxygen and titanium atoms, respectively.

TiO_2 may be divided into three stages over the pressure range. From 15.7 to 40.0 GPa, a-TiO_2 is dominated by 7-fold coordinated baddeleyite-like motifs. Above 40.0 GPa, the fraction of 9-fold coordinated cotunnite-like motifs increases with pressure to become the dominant component at 70.2 GPa. Above 70.2 GPa, it is dominantly in 9-fold coordinated up to the highest pressure of 85.7 GPa in this study, displaying a plateau.

To understand the plateau at CN ≈ 9 above 70.2 GPa, we examine both crystalline and amorphous structures of TiO_2. We note that, unlike the 7-fold coordinated baddeleyite, there are two 9-fold coordinated polymorphs (cotunnite and Fe_2P) that have similar calculated enthalpies (the difference is <0.1 eV/f.u. at 0 K)[25,26] and are stable over a very wide range of pressure (35−636 GPa).[26] It has been proposed in AB binary compounds[27] that the dense packing configuration strongly depends on the ratio (γ) of the ionic radii of the A (r_A) and B (r_B) atoms. We also note that the structural features of local maxima of densely packed binary hard spheres with varying γ depend on the CN of the A atoms. Kummerfeld's study[27] provides an inspiration for correlating pressure-induced CN changes of both crystalline and amorphous materials. To investigate the relationship between CN and $\gamma = r_A/r_O$ in TiO_2, we use simulation results of known TiO_2 polymorphs, namely, rutile (CN = 6), baddeleyite (CN = 7), cotunnite (CN = 9), and Fe_2P (CN = 9),[22,25] under different pressures, and then calculate the γ values of these polymorphs by using the mean fictive ionic radius (MEFIR) method,[28] which weighs shorter bond distances more than longer bond distances. As shown in Figure 3b, within any given crystalline polymorph, γ only exhibits a slight increase (~0.0002 GPa^{-1}) upon compression. However, across different polymorphs, γ changes rapidly: ~0.61 for baddeleyite, ~0.69 for cotunnite, ~0.72 for Fe_2P type 1, and ~0.74 for Fe_2P type 2. Thus, the ratio γ may provide a key to understanding the CN ≈ 9 plateau of a-TiO_2.

We assume that the r_O in a-TiO_2 is the same as that of crystalline polymorphs in the corresponding pressure ranges.[22] The r_O values for the baddeleyite TiO_2 at 15.7−25.8 GPa and cotunnite TiO_2 at 55.0−85.7 GPa may be expressed by a linear relation (Figure S2). This linear relation is also consistent with a simulation study that shows that the O−O distance of a-TiO_2 exhibits a nearly linear shift.[19] By applying this r_O relation to a-TiO_2, we calculate $r_{Ti} = r_{Ti-O} - r_O$ based on our $g(r)$ results. The obtained γ value is 0.614 at 15.7 GPa, which is similar to that of baddeleyite TiO_2 (Figure 3b). At 70.2 GPa, γ is 0.701, similar to that of cotunnite TiO_2. In the pressure range of 15.7−70.2 GPa, the increase in γ is mainly due to the increase in CN, which results in a significant increase in r_{Ti}. At pressures of >70.2 GPa, γ of a-TiO_2 increases continuously from 0.701 to 0.732, a value between that of Fe_2P type 1 ($\gamma \approx 0.72$) and Fe_2P type 2 ($\gamma \approx 0.74$).

DOI: 10.1021/acs.jpclett.9b03378
J. Phys. Chem. Lett. 2020, 11, 374−379

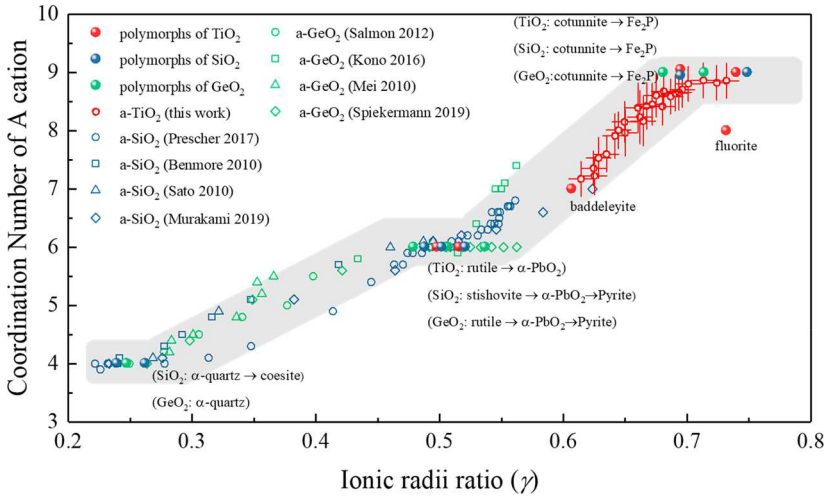

Figure 4. Relationship between the ionic radius ratio and the coordination number of cations. The data of a-AO_2 (empty symbols) are compared with those of crystalline polymorphs (filled circles) with different coordinated structures.

If the structural motifs of a-TiO_2 are assumed to be similar to those of crystalline polymorphs at the corresponding pressures, the above comparisons of γ values provide a hint about the origin of the CN ≈ 9 plateau. The geometric features of different coordination motifs are shown in Figure 3c. For a cotunnite-type polyhedron, the two longest bonds (colored black) are ∼18% longer than the mean Ti−O distance. Thus, cotunnite may be viewed as a (7+2) coordinated structure with a TiO_7 polyhedron modified from baddeleyite-type and two other secondary oxygen ions. Under compression, a cotunnite-type polyhedron may undergo continuous modifications from (7+2) coordination to a more uniform TiO_9 Fe_2P-type polyhedron. As shown in Figure 3b, even though γ continues to increase with pressure above 70.2 GPa, the basic coordination motifs in a-TiO_2 remain a configuration with CN ∼ 9, thus forming a coordination plateau. With further compression, a-TiO_2 may transform to a higher CN with other structural motifs (such as one similar to the *I*4/*mmm* phase with CN = 10).[26]

Finally, to examine the applicability of the relationship mentioned above to a-AO_2 (A = Ti, Si, or Ge), we calculate γ values for them[4,5,8,10−12,14,15] and associated crystalline polymorphs [α-quartz, coesite (CN = 4), rutile/stishovite, α-PbO_2, pyrite (CN = 6), cotunnite, and Fe_2P (CN = 9)] of SiO_2[29−32] and GeO_2[25,29,33] by the MEFIR method. All three compounds, regardless of whether they are crystalline and amorphous, show remarkably consistent behavior (Figure 4). CNs of the A cations exhibit plateaus at CN values of 4, 6, and 9 over wide ranges of γ. For crystalline materials, each of these plateaus is associated with at least two polymorphs over the γ range. The CN of amorphous materials follows closely these plateaus. Between the plateaus, the CN of amorphous materials increases gradually and almost linearly. This CN−γ relationship for a-AO_2 shows that the local structure change in a-AO_2 is closely related to the pressure-induced AO_2 crystalline polymorphs. These data imply a unified relationship between CN and γ in a-AO_2. The existence of 9-fold coordinated a-TiO_2 and the plateau at CN ≈ 9 strongly suggests that similar amorphous structures and plateau may exist in a-SiO_2 and a-GeO_2 at higher pressures. Furthermore, the CN of many forms of a-AO_2 under high pressure is often difficult to determine experimentally, but values of r_{A-O} can be directly obtained from the first peak position in $g(r)$. Thus, the CN in a-AO_2 may be inferred by using the CN−γ relationship.

■ ASSOCIATED CONTENT

Supporting Information

The Supporting Information is available free of charge at https://pubs.acs.org/doi/10.1021/acs.jpclett.9b03378.

Details of the experimental and analytical methods (PDF)

■ AUTHOR INFORMATION

Corresponding Authors

*E-mail: kono.yoshio.rj@ehime-u.ac.jp.
*E-mail: gyshen@anl.gov.

ORCID

Yu Shu: 0000-0002-0903-435X
Quanjun Li: 0000-0002-4718-4156
Changyong Park: 0000-0002-3363-5788
Guoyin Shen: 0000-0001-5146-1147

Present Address

⊥Y.K.: Geodynamics Research Center, Ehime University, Ehime 790-8577, Japan.

Notes

The authors declare no competing financial interest.

■ ACKNOWLEDGMENTS

This research is supported by the National Science Foundation (NSF) under Grant EAR-1722495 (Y.K. and G.S.) and the Department of Energy (DOE), Office of Science/Division of Materials Science and Engineering, under Award DE-FG02-99ER45775 (G.S.). Y.W. acknowledges NSF Grant EAR-1620548. High-pressure experiments were performed at HPCAT (Sector 16), Advanced Photon Source (APS), Argonne National Laboratory. HPCAT operations are supported by DOE-NNSA's Office of Experimental Sciences. The Advanced Photon Source is a U.S. Department of Energy (DOE) Office of Science User Facility operated for the DOE Office of Science by Argonne National Laboratory under Contract DE-AC02-06CH11357. We thank the helpful discussion with Clemens Prescher in the calculations of coordination number.

DOI: 10.1021/acs.jpclett.9b03378
J. Phys. Chem. Lett. 2020, 11, 374−379

REFERENCES

(1) Deb, S. K.; Wilding, M.; Somayazulu, M.; McMillan, P. F. Pressure-Induced Amorphization and an Amorphous−amorphous Transition in Densified Porous Silicon. *Nature* **2001**, *414*, 528.

(2) McMillan, P. F.; Wilson, M.; Daisenberger, D.; Machon, D. A Density-Driven Phase Transition Between Semiconducting and Metallic Polyamorphs of Silicon. *Nat. Mater.* **2005**, *4*, 680−4.

(3) Kohara, S.; Suzuya, K. Intermediate-range Order in Vitreous SiO_2 and GeO_2. *J. Phys.: Condens. Matter* **2005**, *17*, S77−S86.

(4) Benmore, C. J.; Soignard, E.; Amin, S. A.; Guthrie, M.; Shastri, S. D.; Lee, P. L.; Yarger, J. L. Structural and Topological Changes in Silica Glass at Pressure. *Phys. Rev. B: Condens. Matter Mater. Phys.* **2010**, *81*, 054105.

(5) Sato, T.; Funamori, N. High-pressure Structural Transformation of SiO_2 Glass Up to 100 GPa. *Phys. Rev. B: Condens. Matter Mater. Phys.* **2010**, *82*, 184102.

(6) Zeidler, A.; Wezka, K.; Rowlands, R. F.; Whittaker, D. A.; Salmon, P. S.; Polidori, A.; Drewitt, J. W.; Klotz, S.; Fischer, H. E.; Wilding, M. C.; Bull, C. L.; Tucker, M. G.; Wilson, M. High-pressure Transformation of SiO_2 Hlass from a Tetrahedral to an Octahedral Network: a Joint Approach Using Neutron Diffraction and Molecular Dynamics. *Phys. Rev. Lett.* **2014**, *113*, 135501.

(7) Guthrie, M.; Tulk, C. A.; Benmore, C. J.; Xu, J.; Yarger, J. L.; Klug, D. D.; Tse, J. S.; Mao, H. K.; Hemley, R. J. Formation and Structure of a Dense Octahedral Glass. *Phys. Rev. Lett.* **2004**, *93*, 115502.

(8) Mei, Q.; Sinogeikin, S.; Shen, G.; Amin, S.; Benmore, C. J.; Ding, K. High-Pressure x-ray Diffraction Measurements on Vitreous GeO_2 Under Hydrostatic Conditions. *Phys. Rev. B: Condens. Matter Mater. Phys.* **2010**, *81*, 174113.

(9) Hong, X.; Ehm, L.; Duffy, T. S. Polyhedral Units and Network Connectivity in GeO_2 glass at High Pressure: an x-ray Total Scattering Investigation. *Appl. Phys. Lett.* **2014**, *105*, 081904.

(10) Salmon, P. S.; Drewitt, J. W. E.; Whittaker, D. A. J.; Zeidler, A.; Wezka, K.; Bull, C. L.; Tucker, M. G.; Wilding, M. C.; Guthrie, M.; Marrocchelli, D. Erratum: Density-driven Structural Transformations in Network Forming Glasses: a high-pressure Neutron Diffraction Study of GeO_2 Glass Up to 17.5 GPa. *J. Phys.: Condens. Matter* **2012**, *24*, 439601.

(11) Kono, Y.; Kenney-Benson, C.; Ikuta, D.; Shibazaki, Y.; Wang, Y.; Shen, G. Ultrahigh-Pressure Polyamorphism in GeO_2 Glass with Coordination Number> 6. *Proc. Natl. Acad. Sci. U. S. A.* **2016**, *113*, 3436−3441.

(12) Prescher, C.; Prakapenka, V. B.; Stefanski, J.; Jahn, S.; Skinner, L. B.; Wang, Y. Beyond Sixfold Coordinated Si in SiO_2 Glass at Ultrahigh Pressures. *Proc. Natl. Acad. Sci. U. S. A.* **2017**, *114*, 10041−10046.

(13) Petitgirard, S.; Sahle, C.; Weis, C.; Gilmore, K.; Spiekermann, G.; Tse, J.; Wilke, M.; Cavallari, C.; Cerantola, V.; Sternemann, C. Magma Properties at Deep Earth's Conditions from Electronic Structure of Silica. *Geochem. Persp. Lett.* **2019**, *9*, 32−37.

(14) Spiekermann, G.; Harder, M.; Gilmore, K.; Zalden, P.; Sahle, C. J.; Petitgirard, S.; Wilke, M.; Biedermann, N.; Weis, C.; Morgenroth, W.; et al. Persistent Octahedral Coordination in Amorphous GeO_2 Up to 100 GPa by K β'' X-Ray Emission Spectroscopy. *Phys. Rev. X* **2019**, *9*, 011025.

(15) Murakami, M.; Kohara, S.; Kitamura, N.; Akola, J.; Inoue, H.; Hirata, A.; Hiraoka, Y.; Onodera, Y.; Obayashi, I.; Kalikka, J.; et al. Ultrahigh-pressure Form of SiO_2 Glass with Dense Pyrite-Type Crystalline Homology. *Phys. Rev. B: Condens. Matter Mater. Phys.* **2019**, *99*, 045153.

(16) Leger, J. M.; Haines, J.; Pereira, A. S. Structural Investigations Under High Pressure. *Koatsuryoku no Kagaku to Gijutsu* **1998**, *7*, 295−297.

(17) Li, Q.; Liu, B.; Wang, L.; Li, D.; Liu, R.; Zou, B.; Cui, T.; Zou, G.; Meng, Y.; Mao, H.-k.; Liu, Z.; Liu, J.; Li, J. Pressure-Induced Amorphization and Polyamorphism in One-Dimensional Single-Crystal TiO_2 Nanomaterials. *J. Phys. Chem. Lett.* **2010**, *1*, 309−314.

(18) Machon, D.; Daniel, M.; Pischedda, V.; Daniele, S.; Bouvier, P.; LeFloch, S. Pressure-Induced Polyamorphism In TiO_2 Nanoparticles. *Phys. Rev. B: Condens. Matter Mater. Phys.* **2010**, *82*, 140102.

(19) Durandurdu, M. Two Successive Amorphous-to-Amorphous Phase Transformations in TiO_2. *J. Am. Ceram. Soc.* **2017**, *100*, 3903−3911.

(20) Kono, Y.; Park, C.; Kenney-Benson, C.; Shen, G.; Wang, Y. Toward Comprehensive Studies of Liquids at High Pressures and High Temperatures: Combined Structure, Elastic Wave Velocity, and Viscosity Measurements in the Paris−Edinburgh Cell. *Phys. Earth Planet. Inter.* **2014**, *228*, 269−280.

(21) Yang, K.; Kachmar, A.; Wang, B.; Krishnan, N. A.; Balonis, M.; Sant, G.; Bauchy, M. New Insights into the Atomic Structure of Amorphous TiO_2 Using Tight-Binding Molecular Dynamics. *J. Chem. Phys.* **2018**, *149*, 094501.

(22) Nishio-Hamane, D.; Shimizu, A.; Nakahira, R.; Niwa, K.; Sano-Furukawa, A.; Okada, T.; Yagi, T.; Kikegawa, T. The Stability and Equation of State for the Cotunnite Phase of TiO_2 Up to 70 GPa. *Phys. Chem. Miner.* **2010**, *37*, 129−136.

(23) Shannon, R. D. Revised Effective Ionic Radii and Systematic Studies of Interatomic Distances in Halides and Chalcogenides. *Acta Crystallogr., Sect. A: Cryst. Phys., Diffr., Theor. Gen. Crystallogr.* **1976**, *32*, 751−767.

(24) Narten, A. Diffraction Pattern and Structure of Noncrystalline BeF_2 and SiO_2 at 25 C. *J. Chem. Phys.* **1972**, *56*, 1905−1909.

(25) Dekura, H.; Tsuchiya, T.; Kuwayama, Y.; Tsuchiya, J. Theoretical and Experimental Evidence for a New Post-Cotunnite Phase of Titanium Dioxide with Significant Optical Absorption. *Phys. Rev. Lett.* **2011**, *107*, 045701.

(26) Lyle, M. J.; Pickard, C. J.; Needs, R. J. Prediction of 10-Fold Coordinated TiO_2 and SiO_2 Structures at Multimegabar Pressures. *Proc. Natl. Acad. Sci. U. S. A.* **2015**, *112*, 6898−6901.

(27) Kummerfeld, J. K.; Hudson, T. S.; Harrowell, P. The Densest Packing of AB Binary Hard-Sphere Homogeneous Compounds Across All Size Ratios. *J. Phys. Chem. B* **2008**, *112*, 10773−10776.

(28) Hoppe, R. Effective Coordination Numbers (ECoN) and Mean Fictive Ionic Radii (MEFIR). *Zeitschrift für Kristallographie-Crystalline Materials* **1979**, *150*, 23−52.

(29) Baur, W. H.; Khan, A. A. Rutile-Type Compounds. IV. SiO_2, GeO_2 and a Comparison with Other Rutile-Type Structures. *Acta Crystallogr., Sect. B: Struct. Crystallogr. Cryst. Chem.* **1971**, *27*, 2133−2139.

(30) Zhang, L.; Popov, D.; Meng, Y.; Wang, J.; Ji, C.; Li, B.; Mao, H.-k. In-Situ Crystal Structure Determination of Seifertite SiO_2 at 129 GPa: Studying a Minor Phase Near Earth's Core−Mantle Boundary. *Am. Mineral.* **2016**, *101*, 231−234.

(31) Du, X.; Tse, J. S. Oxygen Packing Fraction and the Structure of Silicon and Germanium Oxide Glasses. *J. Phys. Chem. B* **2017**, *121*, 10726−10732.

(32) Tsuchiya, T.; Tsuchiya, J. Prediction of a Hexagonal SiO_2 Phase Affecting Stabilities of $MgSiO_3$ and $CaSiO_3$ at Multimegabar Pressures. *Proc. Natl. Acad. Sci. U. S. A.* **2011**, *108*, 1252−5.

(33) Prakapenka, V. B.; Dubrovinsky, L. S.; Shen, G.; Rivers, M. L.; Sutton, S. R.; Dmitriev, V.; Weber, H. P.; Le Bihan, T. α−PbO_2-Type High-Pressure Polymorph of GeO_2. *Phys. Rev. B: Condens. Matter Mater. Phys.* **2003**, *67*, 132101.

DOI: 10.1021/acs.jpclett.9b03378
J. Phys. Chem. Lett. 2020, 11, 374−379